Chiral Siderophore Analogs: Ferrioxamines and Their Iron(III) Coordination Properties

Pnina Yakirevitch,[†] Natacha Rochel,[‡] Anne-Marie Albrecht-Gary,*[,‡] Jacqueline Libman,[†] and Abraham Shanzer*[,†]

Department of Organic Chemistry, The Weizmann Institute of Science, Rehovot, Israel, and Laboratoire de Physico-Chimie Bioinorganique, URA 405 du CNRS, EHICS, Strasbourg, France

Received October 30, 1992

This article describes a new family of linear ferrioxamine B analogs. These analogs have been designed to serve as chemical probes of microbial iron(III) uptake systems by forming conformationally unique complexes with iron(III). This target is achieved by (i) prohibiting the formation of trans isomers due to shortened bridges between the hydroxamate groups and (ii) imposing preferentially either the Δ-cis or Λ-cis configuration due to the presence of chiral centers. The preparation of these analogs is realized by oligomerization of three identical monomers via the Merrifield method of synthesis. Each monomer is composed of an amino acid (L-ala, L-leu, L-asp, L-glu, D-glu) and *N*-hydroxy-3-aminopropionic acid that are linked together through the formation of a hydroxamate ion binding group. Some of these analogs, **1–3**, have been found to substitute ferrioxamine B as growth promoter and iron(III) carrier, while others, **4** and **5**, inhibit ferrioxamine B mediated iron(III) uptake. A priori, three parameters may be taken into account when siderophore-mediated microbial iron(III) uptake is considered: (i) iron(III) binding to the siderophore, (ii) the efficiency of transport of the siderophore–iron(III) complex across the membrane, and (iii) iron(III) release. In an attempt to determine which of these three parameters dictate the compounds' microbial activity, we compare their coordination properties in vitro with their overall effectiveness in vivo. Specifically, we examine the complexes' iron(III) release kinetics with CDTA as sensitive indicators of their coordination properties. Iron(III) release is shown to occur by two rate-limiting processes: a bimolecular ligand exchange step and a monomolecular one which measures the inertness of the complex under the given acidic conditions. Both processes show pronounced dependence on the nature of the amino acid (namely its substituents CH_3, *i*-Bu, and CH_2CONEt_2 and chain length). The bulkier the side chain and longer the chain length, the slower the dissociation and iron(III) exchange rates. These observations are rationalized in terms of electronic and stereochemical effects and compared with the data of the natural counterpart. They also enable us to interpret the compounds' activities in vivo, indicate that transport of the siderophore complexes across the membrane is the decisive parameter, and demonstrate the role of conformational subtleties.

Introduction

Siderophores are natural iron(III) carriers that are excreted by microorganisms when grown under iron(III) stress.[1-4] These compounds scavenge the scarcely available iron(III) from the environment and transport it into the cell via the intervention of membrane proteins.[1-6] The basic characteristics of the natural siderophores are thus formation of strong iron(III) complexes and binding of this complex to specific membrane receptors. The natural, nonchiral ferrioxamine B siderophore is of particular importance, as it is the drug of choice for the treatment of iron-(III) overload. Ferrioxamine B is a linear molecule that possesses three hydroxamate groups on a string which are bridged by amide-containing methylene chains. This motive is created by a linear assembly of repeating *N*-hydroxydiamines and succinic or acetic acid residues. Ferrioxamine B represents an extreme case of configurational variability, in that it can form a total of five isomers when binding trivalent metal ions, each as a racemic mixture[7] (Figure 1).

In an attempt to establish whether the ferrioxamine B receptor is capable of geometric discrimination, the isomeric chromium complexes were separated and their efficiency in inhibiting ferrioxamine mediated iron uptake into streptomyces piloses examined.[8] Both the cis and trans isomers were found to have comparable activity.[8] This result may indicate either (i) lack of geometric discrimination by the ferrioxamine B receptor or (ii) failure of the conformationally poorly defined ferrioxamine B complexes to serve as probes. Since siderophore receptors at large have been shown to exert high geometric and even chiral discrimination,[1-6] the second alternative appeared more likely. In an attempt to provide sensitive probes for the structural requirements of the ferrioxamine B receptor, we aimed at synthetic ferrioxamine B analogs that would preferentially (if not exclusively) adopt the cis configuration, exhibit significant chiral preference, and possess minimal conformational freedom, as if freezing out specific conformation of the natural ferrioxamine B–iron(III) complex.

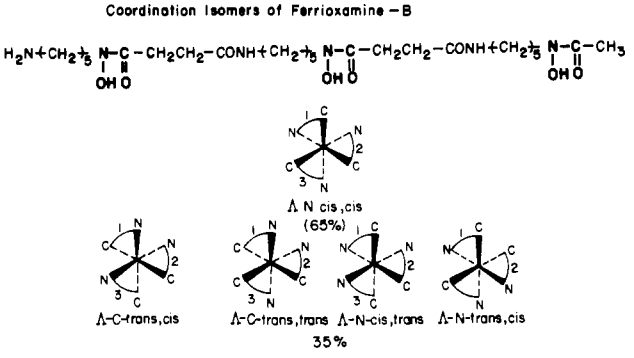

Figure 1. Ferrioxamine B and its isomeric iron(III) complexes.

[†] The Weizmann Institute of Science.
[‡] EHICS.

(1) Neilands, J. B. *Struct. Bonding* **1984**, *58*, 1. Bagg, A.; Neilands, J. B. *Microbiol. Rev.* **1987**, *51*, 509.
(2) Raymond, K. N.; Mueller, G.; Matzanke, B. F. *Top. Cur. Chem.* **1984**, *123*, 49.
(3) Hider, R. C. *Struct. Bonding* **1984**, *58*, 25.
(4) Emery, T. *Met. Ions Biol. Syst.* **1978**, *7*, 77.
(5) *Iron Transport in Microbes, Plants and Animals*; Winkelmann, G., van der Helm, D., Neilands, J. B., Eds.; VCH Verlagsgesellschaft mbH: D-6940 Weinheim, Germany, 1987.
(6) Braun, V. *Enzym. Biol. Membr.* **1985**, *3*, 617.
(7) Leong, J.; Raymond, K. N. *J. Am. Chem. Soc.* **1975**, *97*, 293.
(8) Mueller, G.; Raymond, K. N. *J. Bacteriol.* **1984**, *160*, 304.

0020-1669/93/1332-1779$04.00/0

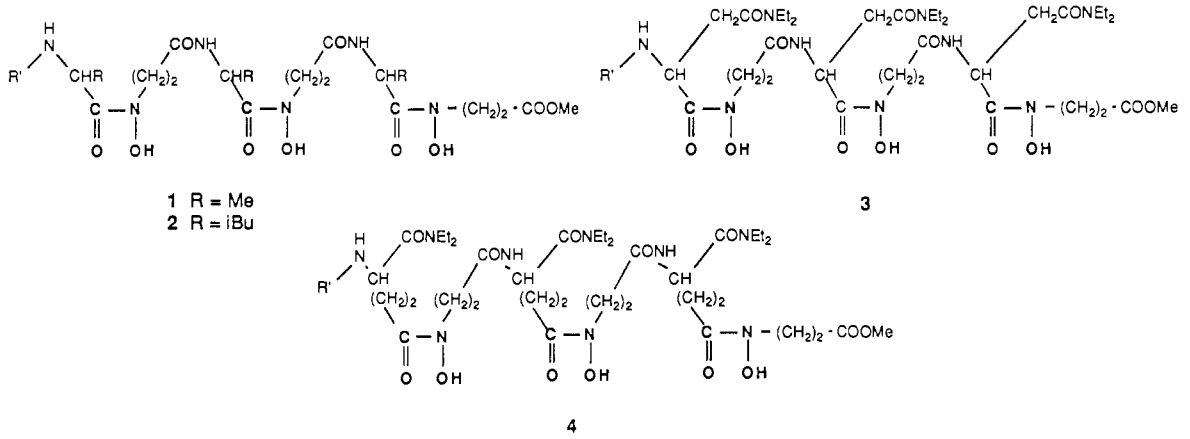

1 R = Me
2 R = iBu

3

4

Figure 2. Biomimetic ferrioxamine B analogs.

Shortening the spacers between the binding sites by replacing the extended chains of ferrioxamine B with α- or γ-amino acid residues was anticipated to reduce the number of possible isomers to those possessing cis geometry, and the incorporation of asymmetric centers to induce chiral preference for either the right- or left-handed cis configuration. The compounds are trimers of three monomeric amino acids, each composed of a natural amino acid linked via a hydroxamate bond to *N*-hydroxyaminopropionic acid. This design greatly facilitates synthesis by relying on natural amino acids as building blocks and the solid-phase method of Merrifield[9] as the preparative method (Figure 2).

These novel binders represent "retro" analogs of the natural siderophores in regard to the directionality of the hydroxamate groups relative to that of the amides. However, biological receptors were anticipated to tolerate this reversal, since earlier studies had shown that retro-ferrichromes equal the activity of the natural siderophore as an iron(III) carrier and growth promoter.[10-12] And indeed, the lower homologs of the series, the ala, leu, and asp derivatives **1–3** proved to substitute ferrioxamine as growth promoter and iron(III) carriers in two types of organisms, *Erwinia herbicola*[13,14] and *Pseudomonas putida*.[15] The higher homologs, however, the glu derivatives **4** (L-glu derivative) and **5** (D-glu derivative) showed different behavior in the two organisms. In *E. herbicola*, **4** and **5** fully simulated ferrioxamine B.[14] In *P. putida*, **4** and **5** merely inhibited ferrioxamine B promoted iron(III) uptake, although with different efficacy. Quite remarkably, **5**, which adopts the Λ configuration when binding iron(III), proved more effective than its enantiomer **4**, which forms the Δ configuration as an iron(III) complex.[15] The latter results demonstrate that the ferrioxamine receptor may exhibit chiral preference for the Λ-cis configuration, in spite of the fact that the natural ferrioxamine B lacks chiral centers.

A priori, three parameters have to be taken into account when siderophore-mediated microbial iron(III) uptake is considered: (i) iron(III) binding to the siderophore, (ii) the efficiency of transport of the siderophore–iron(III) complex across the membrane, and (iii) iron(III) release. The first step, iron(III) uptake, may be assumed to be comparable for all representatives of the series, **1–5**, according to the classical metal-binding Eigen–Winkler mechanism.[16-18] The second step is largely governed by the fit of the siderophore complex to the membrane receptors and transport proteins. Comparison between the overall effectiveness of these compounds and the microbial siderophore *in vivo* and the iron(III) release rates[19-21] was therefore hoped to establish whether transport across the membrane or subsequent iron(III) release govern the microbial activity of these compounds and to which extent conformational differences or coordination properties are determining factors. *In vitro* data on iron(III) release kinetics have the additional advantage of being sensitive indicators for the structural features of the complexes[22,23] in terms of molecular strain and steric hindrance.

Experimental Section

(1) Synthetic Procedures. ^{1}H NMR spectra were measured on the Bruker WH-270 spectrometer (if not stated otherwise) or on the Varian FT-80 spectrometer, at concentrations of (1–2) $\times 10^{-2}$ mol L^{-1}. ^{13}C NMR spectra were measured on a Bruker AMX 400-MHz spectrometer in methanol-d_4 at 2×10^{-2} mol L^{-1}. Chemical shifts are reported in ppm on the δ scale relative to tetramethylsilane (TMS) as an internal standard. Infrared spectra were measured using the Nicolet-510 FTIR spectrometer at concentrations of (1–2) $\times 10^{-2}$ mol L^{-1}. Absorption frequencies are given in cm^{-1}. UV/vis and circular dichroism (CD) spectra were measured using a Hewlett Packard Model 8450A diode array spectrophotometer and a JASCO J-500C spectropolarimeter, respectively.

Fast Atom Bombardment (FAB). Positive FAB mass spectrometry was carried out using a ZAB-HF double-focusing mass spectrometer (mass range 3200 Da at 8 keV ion kinetic energy) and recorded on a VG 11/250 data system (VG Analytical Ltd., Manchester, U.K.). The spectrometer was equipped with a saddle field atom gun (Ion Tech Ltd., Teddington, U.K.). Ionization of the sample was performed with 1 mA of a 8-kV energy Xe atom beam. The matrix was *m*-NBA (Sigma). A 1-μL amount of matrix was deposited on a stainless steel target, and 1 μL of sample solution was added.

Chromatographic purifications were performed by column chromatography, using silica gel 60 (70–230 mesh ASTM) or flash chromatography using silica gel 60 (230–400 mesh ASTM). The homogeneity of the compounds was examined by thin-layer chromatography (mostly

(9) Barany, G.; Merrifield, R. B. In *The Peptides, Analysis, Synthesis, Biology*; Gross, E., Meinhofer, E., Eds.; Academic Press: New York, 1980; Vol. 2, p 1.
(10) Emery, T.; Emery, L.; Olsen, R. K. *Biochem. Biophys. Res. Commun.* **1984**, *119*, 1191.
(11) Tor, Y.; Libman, J.; Shanzer, A. *J. Am. Chem. Soc.* **1987**, *109*, 6518.
(12) Shanzer, A.; Libman, J.; Lazar, R.; Tor, Y.; Emery, T. *Biochem. Biophys. Res. Commun.* **1988**, *157*, 389.
(13) Berner, I.; Yakirevitch, P.; Libman, J.; Shanzer, A.; Winkelmann, G. *Biol. Met.* **1991**, *4*, 186.
(14) Berner, I.; Yakirevitch, P.; Libman, J.; Shanzer, A.; Winkelmann, G. Manuscript in preparation.
(15) Jurkevitch, E.; Chen, Y.; Hadar, Y.; Yakirevitch, P.; Libman, J.; Shanzer, A. Manuscript in preparation.
(16) Eigen, M. *Discuss. Faraday Soc.* **1957**, *24*, 25.
(17) Eigen, M. *Ber. Bunsen-Ges. Phys. Chem.* **1963**, *67*, 753.
(18) Diebler, H.; Eigen, M.; Ilgenfritz, G.; Maas, G.; Winkler, R. *Pure Appl. Chem.* **1969**, *20*, 93.
(19) Monzyk, B.; Crumbliss, A. L. *J. Inorg. Biochem.* **1983**, *19*, 19.
(20) Tufano, T. P.; Raymond, K. N. *J. Am. Chem. Soc.* **1981**, *103*, 6617.
(21) Akiyama, M.; Katoh, A.; Mutoh, T. *J. Org. Chem.* **1988**, *53* (26), 6089.
(22) Albrecht-Gary, A. M.; Dietrich-Buchecker, C.; Saad, Z.; Sauvage, J. P. *J. Am. Chem. Soc.* **1988**, *110*, 1467.
(23) Albrecht-Gary, A. M.; Blanc-Parasote, S.; Boyd, D.; Dauphin, G.; Jeminet, G.; Juillard, J.; Prudhomme, M.; Tissier, C. J. *J. Am. Chem. Soc.* **1989**, *111*, 8598.
(24) (a) Beyerman, H. C.; Hindriks, H.; de Leer, E. W. B. *J. Chem. Soc., Chem. Commun.* **1968**, 1668. (b) *Solid Phase Peptide Synthesis*, 2nd ed.; Stewart, J. M., Young, J. D., Eds.; Pierce Chemical Co.: Rockford, IL, 1984; p 91.

silica-coated plates, Merck), using at least two different solvent systems and two to three visualization methods (i.e. fluorescence quenching, jodine, ninhydrine, $FeCl_3$, etc.).

Solvents and commercially available reagents were of analytical grade. Protected amino acids were purchased from Sigma.

The following abbreviations have been used: Boc = *tert*-butyloxycarbonyl, Bz = benzyl, Ar = aryl, Ph = phenyl, and Et = ethyl.

General Coupling Procedure. To a cold solution of Boc-amino acid (1.0 equiv) were added 1-hydroxybenzotriazole (0.1 equiv) (Fluka) in acetonitrile (dried over basic alumina), amine (1.1 equiv), and *N,N*-diisopropylcarbodiimide (1.1 equiv) (Fluka). The reaction mixture was kept at 0–4 °C for 1–3 h and then at room temperature overnight. The solution was concentrated and the product purified using column chromatography.

General Procedure for Hydrolysis of Monomer Ethyl Ester 7 to Monomer Acid 8. Monomer ethyl ester (1 mmol) was dissolved in methanol (10 mL), and the mixture was treated with 1 M aqueous sodium hydroxide solution (1.25 mL) at room temperature. The reaction mixture was monitored by TLC every 1 h, and additional 1.25-mL portions of aqueous sodium hydroxide solution were added until all starting material has been consumed. The mixture was cooled in an ice bath and acidified with $KHSO_4$ to pH 2. Methanol was evaporated, and the residue was extracted with ethyl acetate. The organic fraction was washed with water, dried on $MgSO_4$, filtered, and concentrated to afford the acid.

General Procedure for Trimerization of Monomers. Trimerization of monomers **8** was carried out using the solid-phase approach. The synthesis was performed manually on chloromethylated polystyrene–2% divinylbenzene resin (Merck). The first monomeric unit was attached to the resin by mixing of monomer (3.4 mmol) in absolute ethanol (14 mL) with triethylamine (0.43 mL, 3 mmol) and polymeric resin (2.3 g) for 72 h at 80 °C. Subsequent coupling steps on the polymeric support were carried out with freshly prepared 1-hydroxybenzotriazole active esters of the monomers in acetonitrile–methylene chloride (85:15) at room temperature over night. The active esters were prepared 2–3 h prior to each coupling step by mixing monomer (2.0 mmol), 1-hydroxybenzotriazole (2.0 mmol), and *N,N*-diisopropylcarbodiimide (2.2 mmol) in acetonitrile at 0 °C.

General Procedure for Cleavage of Trimers from Resin by Transesterification. Cleavage from resin was achieved by transesterification of the trimer with methanol. The resin was suspended in anhydrous methanol (40 mL/1 g of resin), and triethylamine was added (2.6 mL, 18.7 mmol/1 g of resin). The suspension was stirred for 24 h, the polymer was filtered out and washed with methanol, and the solution was concentrated to dryness. Chromatography on silica gel afforded the methyl ester trimer **9**.

***N*-(Benzyloxy)-3-aminopropionic Acid Ethyl Ester (6).** Ethyl acrylate (15.1 g, 16.4 mL, 0.15 mol) was dissolved in 300 mL of ethanol and cooled in a dry-ice–acetone bath. This solution was treated dropwise with a solution of (benzyloxy)amine hydrochloride (12.0 g, 0.075 mol) and triethylamine (10.5 mL, 0.075 mol) in 300 mL of ethanol. The mixture was allowed to warm up to room temperature and stirred for 3 days. The solution was concentrated in vacuo and a mixture of 1:1 hexane–ethyl acetate (20 mL) was added to the slurry. Filtration and chromatography of the filtrate on silica gel (hexane–ethyl acetate, 1:1) provided the benzylated product as an oil, in 40–50% yield. ^{1}H NMR ($CDCl_3$) (80 MHz): δ 7.33 (s, 5H, ArH), 5.75 (br, 1H, NH), 4.69 (s, 2H, CH_2Ph), 4.13 (q, J = 7.1 Hz, 2H, CH_2CH_3), 3.21 (t, J = 6.3 Hz, 2H, CH_2NOBz), 2.56 (t, J = 6.2 Hz, 12H, CH_2CO), 1.24 (t, J = 7.1 Hz, 3H, CH_3). IR ($CDCl_3$): ν 3422 (br, N–H), 1728 (C=O).

L-Alanine-Derived Monomer Ethyl Ester 7a. The ester was prepared according to the general coupling procedure by condensation of Boc-L-alanine (**5a**) and *N*-(benzyloxy)-3-aminopropionic ethyl ester (**6**), followed by column chromatography using 95:5 methylene chloride–ether as eluent, and obtained as an oil. Yield: 54%. ^{1}H NMR ($CDCl_3$) (80 MHz): δ 7.39 (s, 5H, ArH), 4.92 (s, 2H, CH_2Ph), 5.19 (d, 1H, NH), 4.65 (m, 1H, $C_\alpha H$), 4.07 (m, J = 7.1 Hz, 2H, CH_2CH_3), 3.78 (m, 2H, CH_2NOBz), 2.56 (t, J = 6.8 Hz, 2H, CH_2CO), 1.45 (s, 9H, *t*-Bu), 1.27 (d, 3H, J = 6.9 Hz, $C_\alpha HCH_3$), 1.19 (d, 2H, J = 7.2 Hz, CH_2CH_3). IR ($CDCl_3$): ν 3436 (N–H), 1727 (C=O, ester), 1710 (C=O, Boc), 1664 (C=O, CONOBz).

L-Alanine-Derived Monomer 8a. The acid was prepared from the ester **7a** according to the general hydrolysis procedure with 95% yield as oil. ^{1}H NMR ($CDCl_3$): δ 7.38 (s, 5H, ArH), 4.95 (s, 2H, CH_2Ph), 4.24, 3.68 (m, 2H, CH_2NOBz), 2.60 (t, J = 6.7 Hz, 2H, CH_2CO), 1.44 (s, 9H, *t*-Bu), 1.26 (d, 3H, J = 6.9 Hz, CH_3). IR ($CDCl_3$): ν 3434 (N–H), 1713 (C=O, Boc, acid), 1666 (C=O, CONOBz).

L-Alanine-Derived Protected Trimer 9a. Solid-phase synthesis with the L-alanine-derived monomer **8a** and purification by flash chromatography using a gradient of 0–2% methanol in chloroform afforded a white solid, mp 59–62 °C. ^{1}H NMR ($CDCl_3$): δ 7.41, 7.35 (m, 15H, ArH), 6.53 (m, 2H, NH), 4.91 (m, 9H, CH_2Ph (6H) and $C_\alpha H$ (3H)), 4.74 (m, 1H, $C_\alpha H$), 4.19, 3.84 (m, 6H, CH_2NOBz), 3.61 (s, 3H, OCH_3), 2.56, 2.49 (t, 6H, CH_2CO), 1.45 (s, 9H, *t*-Bu), 1.26 (d, 3H, J = 6.8 Hz, CH_3), 1.17 (ft, 6H, CH_3). IR ($CDCl_3$): ν 3429, 3330 (N–H), 1735 (C=O ester), 1711 (C=O, Boc), 1650 (C=O, amide, CONOBz).

L-Alanine-Derived Trimer (1). Hydrogenation of the protected L-alanine-derived trimer **9a** (400 mg, 0.46 mmol) in ethanol (25 mL) with 10% Pd/C (Merck) (200 mg) for 2 h at room temperature and atmospheric pressure, filtration of the catalyst, and evaporation of the solvent afforded the free trishydroxamate ligand in 98% yield. Mp: 184–186 °C. FAB MS: calcd for $C_{24}H_{43}N_6O_{12}$ $(M + H)^+$, m/e 607.28; found, m/e 629.3 $(M + Na)^+$, 607.3 $(M + H)^+$, 507.2 $(M + H - Boc)^+$. ^{1}H NMR ($CDCl_3$–CD_3OD, 7:3) δ 3.95, 3.84 (m, 6H, CH_2NOH), 3.68 (s, 3H, OCH_3), 2.58, 2.49 (m, 6H, CH_2CO), 1.44 (s, 9H, *t*-Bu), 1.17 (ft, 6H, CH_3), 1.12 (d, 3H, J = 6.8 Hz, CH_3). IR ($CDCl_3$): ν 3442, 3314 (N–H), 3150 (O–H), 1734 (C=O ester), 1701 (C=O, Boc), 1627 (sh) (C=O, amide), 1650 (C=O, CONOH).

L-Leucine-Derived Monomer Ester 7b. Applying the general coupling procedure to Boc-L-leucine (**5b**) and *N*-(benzyloxy)-3-aminopropionic ethyl ester **6**, followed by column chromatography using 95:5 methylene chloride–ether provided the ester as an oil in 61% yield. ^{1}H NMR ($CDCl_3$): δ 7.44, 7.37 (m, 5H, ArH), 5.05 (d, J = 9.2, 1H, NH), 4.96 (s, 2H, CH_2Ph), 4.80 (m, 1H, $C_\alpha H$), 4.27, 3.66 (m, 2H, CH_2NOBz), 4.08 (q, J = 7.1, 2H, CH_2CH_3), 2.56 (t, J = 6.8, 2H, CH_2CO), 1.75 (m, 1H, CH(*i*-Bu)), 1.45 (s + m 11H, *t*-Bu, CH_2(*i*-Bu)), 1.20 (t, 3H, J = 7.1, CH_2CH_3), 0.87 (d, 6H, J = 6.6), 0.85 (d, 6H, J = 6.3, CH_3(*i*-Bu)). IR ($CDCl_3$): ν 3438 (N–H), 1724 (C=O ester), 1706 (C=O Boc), 1662 (C=O, CONOBz).

L-Leucine-Derived Monomer Acid 8b. Hydrolysis of ester **7b** according to the general procedure produced the acid in 85% yield. Mp: 146–150 °C. ^{1}H NMR ($CDCl_3$): δ 7.43, 7.36 (m, 5H, ArH), 5.20 (d, J = 9.4, 1H, NH), 4.98 (s, 2H, CH_2CH_3), 4.79 (m, 1H, $C_\alpha H$), 4.28, 3.62 (m, 2H, CH_2NOH), 2.61 (t, J = 6.8, 2H, CH_2CO), 1.68 (m, 1H, CH(*i*-Bu)), 1.45 (s + m 11H, *t*-Bu, CH_2(*i*-Bu)), 0.85 (ft, 6H, CH_3(*i*-Bu)). IR ($CDCl_3$): ν 3437 (N–H), 3300 br (O–H), 1713 (C=O, Boc, acid), 1661 (C=O, CONOBz).

L-Leucine-Derived Protected Trimer 9b. Solid-phase synthesis with the corresponding monomer **8b**, cleavage from the resin according to the general procedure, and chromatography using 97:3 chloroform–methanol as eluent afforded the pure product. Mp: 67–70 °C. ^{1}H NMR ($CDCl_3$): δ 7.48, 7.37 (m, 15H, ArH), 6.39 (m, 2H, NH), 5.15 (m, 3H, NH (1H), $C_\alpha H$ (2H)), 4.96 (m, 6H, CH_2Ph), 4.81 (m, 1H, $C_\alpha H$), 4.26, 3.82 (m, 6H, CH_2NOBz), 3.62 (s, 3H, OCH_3), 2.56 (m, 6H, CH_2CO), 1.67, 1.55 (m, 3H, CH(*i*-Bu)), 1.45 (s, 9H, *t*-Bu, Boc), 1.38 (m, 6H, CH_2(*i*-Bu)), 0.85, 0.78 (m, 18H, CH_3(*i*-Bu)). IR ($CDCl_3$): ν 3423, 3323 (N–H), 1734 (C=O, ester), 1706 (C=O, Boc), 1662 (C=O, amide, CONOBz).

L-Leucine-Derived Trimer (2). Hydrogenation of the protected leucine-derived trimer **9b** in a procedure similar to that for the alanine derivative **9a** using equal weight amounts of the protected trimer and 10% Pd/C afforded the tris/hydroxamate product in 99% yield. Mp: 96–100 °C. FAB MS: calcd for $C_{33}H_{61}N_6O_{12}$ $(M + H)^+$, m/e 733.4; found, 755.5 $(M + Na)^+$, 733.5 $(M + H)^+$, 633.4 $(M + H - Boc)^+$. ^{1}H NMR ($CDCl_3$) revealed broad peaks due to a multitude of conformations. ^{1}H NMR (CD_3OD): δ 3.86 (m, 6H, CH_2NOH), 5.01, 4.78 (m, 3H, $C_\alpha H$), 3.66 (s, 3H, OCH_3), 2.59 (m, 6H, CH_2CO), 1.72 (m, 3H, CH(*i*-Bu)), 1.53 (m, 6H, CH_2(*i*-Bu)), 1.43 (s, 9H, *t*-Bu), 0.93 (m, 18H, CH_3(*i*-Bu)). IR ($CDCl_3$): ν 3442, 3314 (N–H), 3162 (O–H), 1735 (C=O, ester), 1700 (C=O, Boc), 1650 (C=O, CONOH), 1624 (C=O, amide).

***N*-*t*-Boc-L-aspartic Acid β-Diethylamide α-Benzyl Ester.** Condensation of *N*-*t*-Boc-L-aspartic acid α-benzyl ester and diethylamine according to the general coupling procedure, followed by column chromatography using 1:1 hexane–ethyl acetate as eluent, afforded the product as an oil in 80% yield. ^{1}H NMR ($CDCl_3$) (80 MHz): δ 7.31 (s, 5H, ArH), 5.88 (d, 1H, NH), 4.60 (m, 1H, $C_\alpha H$), 3.28 (m, 4H, NCH_2CH_3), 3.05 (dd, J = 4.0, 17.5, 2H, $C_\alpha HCH_2$), 1.41 (s, 9H, *t*-Bu), 1.07 (m, 6H, NCH_2CH_3). IR (neat): ν 3434 (N–H), 1739 (C=O ester), 1716 (C=O, Boc), 1641 (C=O, amide, CONOBz).

***N*-*t*-Boc-L-aspartic Acid β-Diethylamide (5c).** To a solution of *N*-*t*-Boc-L-aspartic acid β-diethylamide α-benzyl ester (3.7 g, 9.8 mmol) in absolute ethanol (80 mL) was added 10% Pd/C (370 mg), and the reaction mixture was hydrogenated for 2.5 h at room temperature and atmospheric

pressure. The catalyst was filtered out and the solvent was evaporated affording the free acid in 97% yield. Mp: 79–84 °C. ^{1}H NMR ($CDCl_3$): δ 5.86 (d, 1H, NH), 4.49 (m, 1H, $C_\alpha H$), 3.40 (m, 4H, NCH_2CH_3), 3.25, 2.69 (m, 2H, $C_\alpha HCH_2$), 1.45 (s, 9H, *t*-Bu), 1.24 (t, 3H, NCH_2CH_3 (cis)), 1.15 (t, 3H, NCH_2CH_3 (trans)). IR ($CDCl_3$): ν 3421 (N–H), 1704 (C=O, Boc, acid), 1640 (C=O, CONOBz), 1583 (C=O, amide).

L-Aspartic Acid Derived Monomer Ethyl Ester 7c. Condensation of *N*-*t*-Boc-L-aspartic acid β-diethylamide (**5c**) and *N*-(benzyloxy)-3-aminopropionic ethyl ester (**6**) according to the general procedure, followed by column chromatography using 1:1 hexane–ethyl acetate as eluent, provided the product as an oil in 61% yield. ^{1}H NMR ($CDCl_3$): δ 7.45, 7.36 (m, 5H, ArH), 5.46 (d, *J* = 7.1, 1H, NH), 4.98 (m, 3H, CH_2Ph (2H), $C_\alpha H$ (1H)), 4.07 (3H, q, *J* = 7.1, (2H), OCH_2CH_3, m, (1H) CH_2NOBz), 3.85 (m, 1H, CH_2NOBz), 3.31 (q, 2H, NCH_2CH_3 (trans)), 3.20 (m, 2H, NCH_2CH_3 (cis)), 2.82, 2.62 (m, 4H, CH_2COOEt, $C_\alpha CH_2$CO), 1.43 (s, 9H, *t*-Bu), 1.19, 1.08 (m, 9H, OCH_2CH_3, NCH_2CH_3). IR ($CDCl_3$): ν 3433 (N–H), 1724 (C=O ester, Boc), 1635 (C=O, amide, CONOBz).

L-Aspartic Acid Derived Monomer Acid 8c. Hydrolysis of **7c** according to the general hydrolysis procedure provided the product as an oil in 85% yield. ^{1}H NMR ($CDCl_3$): δ 7.41, 7.37 (m, 5H, ArH), 5.51 (d, *J* = 6.9, 1H, NH), 4.97, 4.83 (Abq, *J* = 9.9, 37.4, 2H, CH_2Ph), 4.40 (m, 1H, $C_\alpha H$), 4.25, 3.71 (m, 2H, CH_2NOBz), 3.25 (m, 4H, CH_2CH_3), 2.78, 2.55 (m, 4H, CH_2COOH, $C_\alpha CH_2$CO), 1.44 (s, 9H, *t*-Bu), 1.11 (m, 3H, CH_3 (cis)), 1.01 (m, 3H, CH_3 (trans)). IR ($CDCl_3$): ν 3422 (N–H), 1712 (C=O Boc, acid), 1664 (C=O, CONOBz), 1633 (C=O, amide).

L-Aspartyl-Derived Protected Trimer 9c. Solid-phase synthesis from the L-aspartyl-derived monomer **8c** and purification on flash chromatography using a gradient of 0.5–1.5% methanol in chloroform afforded the product as an oil. ^{1}H NMR ($CDCl_3$): δ 7.52, 7.33 (m, 15H, ArH), 5.15, 5.05 (m, 3H, $C_\alpha H$), 5.52 (br, 2H, NH), 5.37 (d, 1H, NH), 4.95, 4.80 (m, 6H, CH_2Ph), 4.08, 3.83 (m, 6H, CH_2NOBz), 3.58 (s, 3H, OCH_3), 3.37, 3.25, 3.00 (m, 12H, NCH_2CH_3), 2.68 (m, 12H, CH_2COOCH_3, $C_\alpha CH_2$CO), 1.44 (s, 9H, *t*-Bu), 1.14, 1.01 (m, 18H, NCH_2CH_3). IR ($CDCl_3$): ν 3434, 3319 (N–H), 1721 (sh) (C=O ester), 1705 (C=O, Boc), 1655 (C=O, CONOBz), 1629 (C=O, amide).

L-Aspartyl-Derived Trimer 3. Hydrogenation of the protected aspartyl trimer **9c** in a procedure similar to that for the alanine derivative **9a** afforded the trishydroxamate product with 99% yield as an oil. FAB MS: calcd for $C_{39}H_{70}N_9O_{15}$ $(M + H)^+$, *m/e* 904.49; found, *m/e* 926.5 $(M + Na)^+$, 904.5 $(M + H)^+$, 804.5 $(M + H - Boc)^+$. ^{1}H NMR ($CDCl_3$): 10.79 (br, 1H, OH), 10.39 (br, 2H, OH), 7.48 (d, *J* = 6.0, 1H, NH), 7.31 (d, *J* = 6.4, 1H, NH), 5.66 (br, *J* = 6.4, 1H, NH), 5.36, 5.26, 5.09 (m, 3H, $C_\alpha H$), 4.14, 3.92 (m, 6H, CH_2NOH), 3.67 (s, 3H, OCH_3), 3.32 (m, 12H, NCH_2CH_3), 2.95, 2.85 (m, 6H, CH_2CO), 2.66, 2.56, 2.43 (m, 6H, $C_\alpha CH_2$CO), 1.42 (s, 9H, *t*-Bu), 1.18, 1.10 (m, 18H, NCH_2CH_3). IR ($CDCl_3$): ν 3420, 3312 (N–H), 1734 (sh) (C=O ester), 1704 (C=O, Boc), 1632 (C=O, CONOH, amide).

***N*-*t*-Boc-L-glutamic Acid α-Diethylamide γ-Benzyl Ester.** Condensation of *N*-*t*-Boc-L-glutamic acid γ-benzyl ester and diethylamine according to the general coupling procedure, followed by column chromatography using 1:1 hexane–ethyl acetate as eluent, provided the product in 50–60% yield as an oil. ^{1}H NMR ($CDCl_3$): δ 7.36 (m, 5H, ArH), 5.40 (d, *J* = 8.6, 1H, NH), 5.13, 5.14 (s, 2H, CH_2Ph), 4.64 (m, 1H, $C_\alpha H$), 3.51, 3.30 (m, 4H, NCH_2CH_3), 2.47 (m, 2H, CH_2CO), 2.03, 1.74 (m, 2H, $C_\alpha HCH_2$), 1.42 (s, 9H, *t*-Bu), 1.22 (t, *J* = 7.1, 3H, NCH_2CH_3 (cis)), 1.11 (t, *J* = 7.1, 3H, NCH_2CH_3 (trans)). IR ($CDCl_3$): ν 3425 (N–H), 1729 (C=O ester), 1705 (C=O, Boc), 1637 (C=O, amide).

***N*-*t*-Boc-L-glutamic Acid α-Diethylamide (5d).** To a solution of *N*-*t*-Boc-L-glutamic acid α-diethylamide γ-benzyl ester (1.5 g, 3.8 mmol) in absolute ethanol was added 10% Pd/C (200 mg), and the reaction mixture was hydrogenated for 2 h at room temperature and atmospheric pressure. The catalyst was filtered out and the solvent was evaporated affording the free acid in 80–90% yield. Mp: 138–144 °C. ^{1}H NMR ($CDCl_3$): δ 5.62 (d, *J* = 8.5 Hz, 1H, NH), 4.63 (m, 1H, $C_\alpha H$), 3.51 (m, 2H, NCH_2CH_3 (trans)), 3.25 (m, 4H, NCH_2CH_3 (cis)), 2.44 (m, 2H, CH_2CO), 2.00, 1.70 (m, 2H, $C_\alpha HCH_2$), 1.43 (s, 9H, *t*-Bu), 1.22 (t, *J* = 7.1, 3H, NCH_2CH_3 (cis)), 1.12 (t, *J* = 7.0, 3H, NCH_2CH_3 (trans)). IR ($CDCl_3$): ν 3427 (N–H), 1707 (C=O, Boc, acid), 1636 (C=O, amide).

L-Glutamic Acid Derived Monomer Ethyl Ester 7d. Condensation of *N*-*t*-Boc-L-glutamic acid α-diethylamide (**5d**) and *N*-(benzyloxy)-3-aminopropionic ethyl ester (**6**) according to the general procedure, followed by column chromatography using 1:1 hexane–ethyl acetate as eluent, afforded the acid in 70–85% yield as an oil. ^{1}H NMR ($CDCl_3$): δ 7.38 (s, 5H, ArH), 5.47 (d, *J* = 8.8 Hz, 1H, NH), 4.83 (s, 2H, CH_2Ph), 4.58 (m, 1H, $C_\alpha H$), 4.07 (q, *J* = 7.1, 2H, OCH_2CH_3, m, 1H, CH_2NOBz), 3.90 (m, 1H, CH_2NOBz), 3.65, 3.54, 3.34, 3.22 (m, 4H, NCH_2CH_3), 2.60 (t, *J* = 6.9, 2H, CH_2CO), 2.04, 1.65 (m, 2H, $C_\alpha HCH_2$), 1.39 (s, 9H, *t*-Bu), 1.23 (t, *J* = 7.5, 3H, OCH_2CH_3), 1.20 (t, *J* = 7.1, 3H, NCH_2CH_3 (cis)), 1.11 (t, *J* = 7.1, 3H, NCH_2CH_3 (trans)). IR ($CDCl_3$): ν 3427 (N–H), 1727 (C=O ester), 1705 (C=O, Boc), 1637 (C=O, amide, CONOBz).

L-Glutamic Acid Derived Monomer Acid 8d. Hydrolysis of ester **7d** according to the general hydrolysis procedure afforded the acid in 80–85% yield. Mp: 89–91 °C. ^{1}H NMR ($CDCl_3$): δ 7.37 (s, 5H, ArH), 5.64 (d, *J* = 8.5 Hz, 1H, NH), 4.82 (s, 2H, CH_2Ph), 4.57 (m, 1H, $C_\alpha H$), 4.01, 3.90 (m, 2H, CH_2NOBz), 3.70, 3.53, 3.34, 3.21 (m, 4H, NCH_2CH_3), 2.63 (m, 2H, CH_2CO), 2.04, 1.62 (m, 2H, $C_\alpha HCH_2$), 1.38 (s, 9H, *t*-Bu), 1.23 (t, *J* = 7.0, 3H, NCH_2CH_3 (cis)), 1.11 (t, *J* = 7.1, 3H, NCH_2CH_3 (trans)). IR ($CDCl_3$): ν 3424 (N–H), 1711 (C=O, Boc, COOH), 1636 (C=O, amide, CONOBz).

L-Glutamyl-Derived Protected Trimer 9d. Solid-phase synthesis from the L-glutamyl-derived monomer **8d** and purification on flash chromatography using 97:3 chloroform–methanol afforded the product as an oil. ^{1}H NMR ($CDCl_3$): δ 7.34 (m, 15H, ArH), 6.85 (d, *J* = 8.4, 1H, NH), 6.65 (d, 1H, NH), 5.49 (d, 1H, Boc-N*H*), 4.88 (m, 2H, $C_\alpha H$), 4.78, 4.73 (s, 6H, CH_2Ph), 4.55 (m, 1H, $C_\alpha H$), 3.91, 3.52, 3.31, 3.14 (m, 18H, CH_2NOBz, NCH_2CH_3), 3.61 (s, 3H, OCH_3), 2.56 (m, 12H, CH_2CO), 2.0, 1.71 (m, 6H, $C_\alpha HCH_2$), 1.38 (s, 9H, *t*-Bu), 1.19 (m, 9H, NCH_2CH_3 (cis)), 1.08 (m, 9H, NCH_2CH_3 (trans)). IR ($CDCl_3$): ν 3417, 3340 (N–H), 1736 (C=O ester), 1704 (C=O, Boc), 1636 (C=O, amide, CONOBz).

L-Glutamyl-Derived Trimer 4. Hydrogenation of the protected glutamyl trimer **9d** in a procedure similar to that for the alanine derivative **9a** afforded the trishydroxamate product **4** in 91% yield. Mp: 61–68 °C. FAB MS: calcd for $C_{42}H_{76}N_9O_{15}$ $(M + H)^+$, *m/e* 946.5; found, *m/e* 968.4 $(M + Na)^+$, 946.5 $(M + H)^+$, 846.4 $(M + H - Boc)^+$. ^{1}H NMR ($CDCl_3$) revealed broad picks due to a multitude of conformations. ^{1}H NMR (CD_3OD): δ 5.22 (m, 2H, $C_\alpha H$), 3.87 (m, 6H, CH_2NOH), 3.66 (s, 3H, OCH_3), 3.46, 3.24 (m, 12H, NCH_2CH_3), 2.59 (m, 12H, CH_2CO), 1.98, 1.78 (m, 6H, $C_\alpha HCH_2$), 1.42 (s, 9H, *t*-Bu), 1.26 (t, *J* = 6.9 Hz, 9H, NCH_2CH_3 (cis)), 1.11 (t, *J* = 7.1 Hz, 9H, NCH_2CH_3 (trans)). IR ($CDCl_3$): ν 3408, 3300 (N–H), 1735 (C=O ester), 1701 (sh) (C=O, Boc), 1635 (C=O, amide, CONOH).

(2) Kinetic Measurements. Cyclohexylene-1,2-dinitrilotetraacetate (CDTA, Titriplex IV, Merck, pa) was chosen as a scavenger for the dissociation of the iron(III) complexes,[25,26] since CDTA is soluble in aqueous methanol at concentrations up to ten times in excess of that of the iron(III) complexes (~10^{-4} mol L^{-1}). A methanol–water mixture (80:20 by volume) was used as solvent, since it solubilizes the reactants and products of the global ligand-exchange reaction:

$$LFe^{III} + CDTA \rightarrow (CDTA)Fe^{III} + L \qquad (1)$$

L = various free ligands

The stock solutions of iron(III) ($FeCl_3$, $6H_2O$, Merck, pa) were titrated by classical methods.[27] The acidity of the medium was fixed with an acetate buffer (10^{-1} mol L^{-1}) to a value of –log $[H^+]$ = 6.3 ± 0.1 by mixing CH_3COONa (Fluka, pa) with $HClO_4$ acid (Merck, pa) in appropriate proportions. The ionic strength (0.1) was maintained constant by the buffer concentration. The –log $[H^+]$ values were determined by a combined microelectrode (Tacussel) and a voltameter (Tacussel, Isis 20 000). The microelectrode was filled with a solution of NaCl (Merck, pa, 5×10^{-2} mol L^{-1}) and $NaClO_4$ (Merck, pa, 5×10^{-2} mol L^{-1}). The linearity of the glass electrode was verified[28,29] using perchloric acid (Prolabo, Normapur) solutions (~10^{-2} mol L^{-1}), oxalate [2×10^{-2} mol L^{-1} oxalic acid (Prolabo) and 1×10^{-2} mol L^{-1} ammonium oxalate (Prolabo); –log $[H^+]$ = 3.1] and succinate [2×10^{-2} mol L^{-1} succinic acid (Prolabo) and 1×10^{-2} mol L^{-1} lithium methylate; –log $[H^+]$ = 6.0] buffers. The concentrations of CDTA were varied between 10^{-3} mol L^{-1} and 7×10^{-3} mol L^{-1}. The concentrations of all the iron(III) complexes, including those of ferrioxamine B, were in the range of 9.5×10^{-5} mol L^{-1} to 1.2×10^{-4} mol L^{-1}. The formation curves of protonated CDTA

(25) Pausch, J. B.; Margerum, D. W. *Anal. Chem.* **1969**, *41* (2), 226.
(26) Margerum, D. W.; Pausch, J. B.; Nyssen, G. A.; Smith, G. F. *Anal. Chem.* **1969**, *41* (2), 233.
(27) Theis, M. Z. *Analyt. Chem.* **1955**, *144*, 351.
(28) De Ligny, C. L.; Luykx, P. F. M.; Rehbach, M.; Wieneke, A. A. *Recl. Trav. Chim. Pays-Bas* **1960**, *79*, 713.
(29) Alfenaar, M.; De Ligny, C. L. *Recl. Trav. Chim. Pays-Bas* **1967**, *86*, 1185.

Table I. Extinction Coefficients of the Synthetic Iron(III) Trishydroxamate Complexes and of Ferrioxamine B[a]

complexes	λ_{max} (nm)	ϵ_{max} (mol^{-1} L cm^{-1})	complexes	λ_{max} (nm)	ϵ_{max} (mol^{-1} L cm^{-1})
1–Fe(III)	425	2460 ± 50	**4–Fe(III)**	420	2320 ± 50
2–Fe(III)	423	2120 ± 50	ferrioxamine B	430	2650 ± 50
3–Fe(III)	430	2450 ± 50			

[a] Solvent methanol/water (80:20); $-\log [H^+] = 6.3 \pm 0.1$; $I = 0.1$; $T = 25.0 \pm 0.1$ °C.

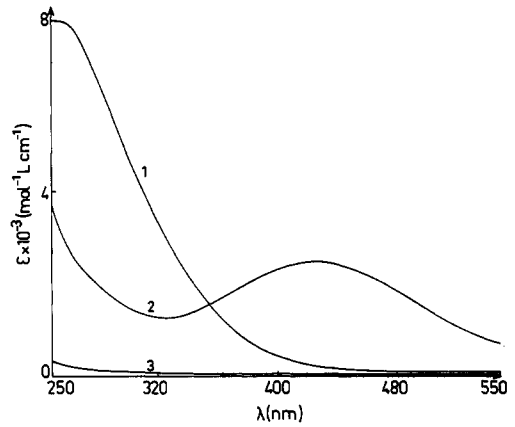

Figure 3. Electronic spectra of the reactants and the products of the **1–Fe(III)** dissociation reaction by CDTA: Solvent methanol/water (80:20); $-\log [H^+] = 6.3 \pm 0.1$; $I = 0.1$; $T = 25.0 \pm 0.1$ °C. Key: (1) $(CDTA)Fe^{III}$; (2) **1–Fe(III)**; (3) free ligand **1**.

at varying values of $-\log [H^+]$ were calculated from literature data[30] for the protonation constants of CDTA in aqueous methanol (80:20 by volume) with the help of the Haltafall program.[31] In our conditions ($-\log [H^+] = 6.3 \pm 0.1$), the diprotonated species and triprotonated species $CDTAH_2^{2-}$ and $CDTAH_3^-$ predominated (55% and 41%, respectively, of the total CDTA concentration). All the protonation equilibria involved in the ligand exchange reactions between the iron(III) complexes and CDTA were considered as fast classical proton exchanges. The kinetics of iron(III) exchange was monitored by absorption spectroscopy at 425 nm (Kontron Uvikon 860) in the region of the charge-transfer absorbance of ferrioxamine B and of the synthetic iron(III) trishydroxamate complexes (Table I).

At this wavelength desferrioxamine B and all the synthetic free ligands do not absorb, and the $(CDTA)Fe^{III}$ complex formed during the reaction 1 does not show a significant absorption ($\epsilon_{425\ nm} = 250 \pm 50$ mol^{-1} L cm^{-1}), as presented in Figure 3.

The data were treated on line by the Biokine program[32] using an IBM PS2 microcomputer and by the software written by Provencher[33] using an IBM computer.

Results and Discussion

The trishydroxamates were prepared in a series of essentially four stages. These involved (i) preparation of the protected amino acid residue, (ii) coupling of the amino acid residue with *N*-(hydroxybenzyl)-3-aminopropionic acid ester to the monomer and removal of the ester protecting groups, (iii) trimerization of the monomers by the Merrifield method,[9,24] and (iv) hydrogenolysis to the free ferrioxamine analogs (Scheme I).

All intermediates and final products were characterized by their spectroscopic and analytical properties, which were in full agreement with the assigned structures. All monomeric esters showed three carbonyl absorptions in the IR spectra (Table II), which correspond to the ester, *tert*-butoxy, and hydroxamate carbonyls around 1725, 1710, and 1660 cm^{-1}, respectively. The high-frequency absorptions of the NH group above 3400 cm^{-1} exclude the presence of H-bonds. The protected, trimeric esters showed a fourth carbonyl absorption around 1640 cm^{-1}, which is assigned to the amide carbonyl, and two NH frequencies, one above 3400 cm^{-1} and one below 3400 cm^{-1}, indicating the presence of both free and bonded NH groups. The NMR spectra (Table III) of the monomeric esters reveal for most cases (except for the asp derivative) a sharp singlet for the benzyloxy protons and two sets of signals for the $NOCH_2$ protons, deriving from cisoid and transoid configurations of the hydroxamate bond. Most indicative for the trimeric derivatives are the ratios between the benzyloxy protons and the *tert*-butoxy and methoxy protons, as there are in each trimer three benzyloxy groups but merely one terminal butoxy and one methoxy group. In addition, the trimers exhibit

Scheme I.

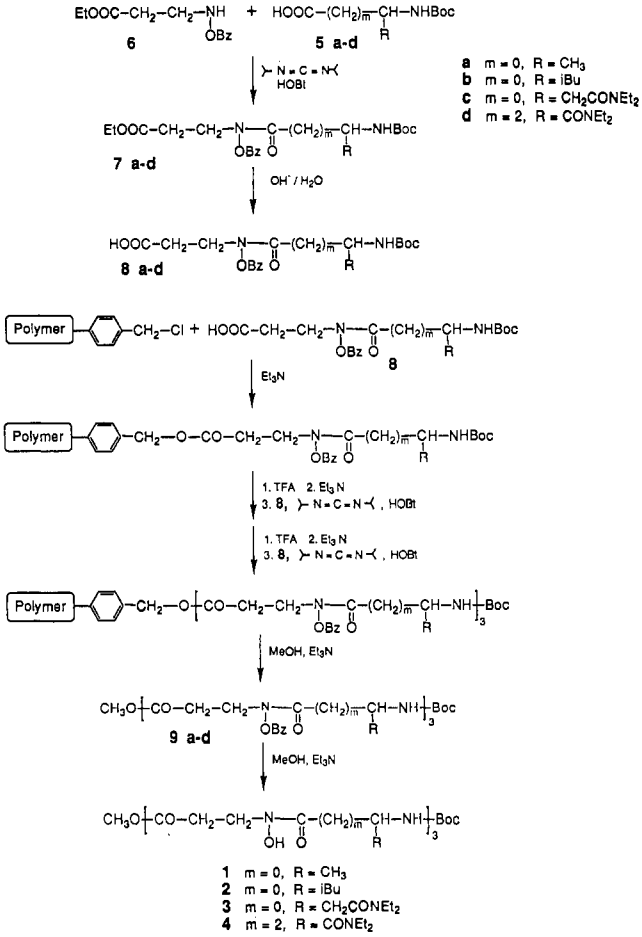

Table II. IR Spectral Data for Ferrioxamine Analogs and Intermediates[a]

compd	ν(N–H) (cm^{-1})	ν(*C*OOR) (cm^{-1})	ν(*t*-BuO*C*O) (cm^{-1})	ν(*C*ONO) (cm^{-1})	ν(*C*ONH) (cm^{-1})
7a	3436	1727	1710	1664	
8a	3434	1713	1713	1666	
9a	3429, 3330 (br)	1735	1711	1650	1650
1	3442, 3314	1734	1701	1650	1627
7b	3438	1724	1706	1662	
8b	3437	1713	1713	1661	
9a	3423, 3323	1734	1706	1656	1656
2	3442, 3314	1735	1700	1650	1624
7c	3433	1724	1724	1635	1635
8c	3422	1712	1712	1664	1633
9c	3434, 3319	1721	1705	1655	1629
3	3420, 3312	1734	1704	1632	1632
7d	3427	1727	1705	1637	1637
8d	3424	1711	1711	1636	1636
9d	3417, 3340 (br)	1736	1704	1636	1636
4	3408, 3300	1735	1701	1635	1635

[a] IR spectra measured in $CDCl_3$ at $(1–2) \times 10^{-2}$ mol L^{-1} concentrations.

(30) Rorabacher, D. B.; MacKellar, W. J.; Shu, F. R.; Bonavita, M. *Anal. Chem.* **1971**, *43* (4), 561.
(31) Ingri, N.; Kakolowics, W.; Sillen, L. G.; Warnquist, B. *Talanta* **1969**, *14*, 1261.
(32) Bio-Kine Software, Biologic, Grenoble, France.
(33) Provencher, S. W. *J. Chem. Phys.* **1976**, *64* (7), 2772.

Table III. ^{1}H-NMR Spectral Data (ppm) for Ferrioxamine Analogs and Intermediates[a]

compd	solvent	*t*-Bu	BocN*H*, CON*H*	$C_\alpha H$	NOC*H*$_2$Ph	NOC*H*$_2$CH$_2$	NOCH$_2$C*H*$_2$	OC*H*$_3$
7a	$CDCl_3$	1.45 (s)	5.19 (d)	4.65 (m)	4.92 (s)	4.07 (m) 3.78 (m)	2.56 (t)	
8a	$CDCl_3$	1.44 (s)	5.42 (d)	4.73 (m)	4.95 (s)	4.24 (m) 3.68 (m)	2.60 (t)	
9a	$CDCl_3$	1.45 (s)	6.53 (m)	4.91 (m) 4.74 (m)	4.91[b]	4.19 (m) 3.84 (m)	2.56 (t) 2.49 (t)	3.61 (s)
1	$CDCl_3$–CD_3OD	1.44 (s)				3.68 (m) 3.54 (m)	2.58 (m) 2.49 (m)	3.68 (s)
7b	$CDCl_3$	1.45 (s)	5.05 (d)	4.80 (m)	4.96 (s)	4.27 (m) 3.66 (m)	2.56 (t)	
8b	$CDCl_3$	1.45 (s)	5.20 (d)	4.79 (m)	4.98 (s)	4.28 (m) 3.62 (m)	2.61 (t)	
9b	$CDCl_3$	1.45 (s)	6.39 (m)	5.15 (m) 4.81 (m)	4.96[b]	4.26 (m) 3.62 (m)	2.56 (m)	3.62 (s)
2	CD_3OD	1.43 (s)		5.01 (m) 4.78 (m)		3.86 (m)	2.59 (m)	3.66 (s)
7c	$CDCl_3$	1.43 (s)	5.46 (d)	4.40 (m)	4.98[b]	4.07 (m)	2.82 (m) 2.62 (m)	
8c	$CDCl_3$	1.44 (s)	5.51 (d)	4.40 (m)	4.98; 4.83 (ABq)	4.25 (m) 3.71 (m)	2.78 (m) 2.55 (m)	
9c	$CDCl_3$	1.44 (s)	5.52 (br) 5.37 (d)	5.15 (m) 5.05 (m)	4.95; 4.80[b]	4.08 (m) 3.83 (m)	2.68 (m)	3.58 (s)
3	$CDCl_3$	1.42 (s)	7.48 (d) 7.31 (d) 5.66 (d)	5.36 (m) 5.26 (m) 5.09 (m)		4.14 (m) 3.92 (m)	2.95 (m) 2.85 (m)	3.67 (s)
7d	$CDCl_3$	1.39 (2)	5.47 (d)	4.58 (m)	4.83 (s)	4.07 (m) 3.90 (m)	2.60 (m)	
8d	$CDCl_3$	1.38 (s)	5.64 (d)	4.57 (m)	4.82 (s)	4.01 (m) 3.90 (m)	2.63 (m)	
9d	$CDCl_3$	1.38 (s)	6.85 (d) 6.65 (d) 5.49 (d)	4.88 (m) 4.55 (m)	4.78 (s) 4.73 (s)	3.91 (m) 3.52 (m)	2.56 (m)	3.61 (s)
4	CD_3OD	1.42 (s)		5.22 (m)		3.87 (m)	2.59 (m)	3.66 (s)

[a] Spectra measured at (1–2) × 10^{-2} mol L^{-1} concentrations. [b] Several signals.

several benzyloxy signals since each of the units is in a different environment, while the two multiplets for the NOCH$_2$– protons are retained. Some of the C_α protons in the trimeric esters shift to lower fields relative to the corresponding protons in the monomers, and some of the amide protons resonate at rather low fields. This is indicative of H-bonded amides, in compliance with the low-frequency IR data.

Further support for the structural assignments of the ferrioxamine analogs **1–5** was obtained by high-resolution FAB mass spectrometry and ^{13}C-NMR spectroscopy. The FAB spectra showed signals corresponding to the sodium complex of the ligands $(M + Na)^+$, as well as signals derived from the protonated molecule $(M + H)^+$ and the protonated molecule after loss of the butoxy group $(M + H - Boc)^+$. The ^{13}C-NMR spectra of the ferrioxamine analogs **1–4** are summarized in Table IV. The spectra never showed more than three sets of signals corresponding to each of the monomeric subunits, indicating the presence of single isomers. The assignments of the individual signals are based on comparison between the four representatives of the series, **1–4**, and on comparison with literature data on the respective amino acid residues, alanine, leucine, and aspartic and glutamic acids.[34]

Titration with $FeCl_3$ in aqueous methanol buffer established 1:1 ion binding stoichiometry for all compounds, and CD spectroscopy of the iron(III) complexes demonstrated preferred right handedness (Figure 4)[35] when L-amino acids were used as components.

Quite remarkably, the extent of chiral preference for the Δ-cis configuration when L-amino acids were used varied substantially with the nature of the amino acid.[36] While the chiral preference was small for the ala and leu derivatives **1** and **2**, it was larger for the asp derivative **3** and particularly large for the glu derivatives **4** and **5**. The enhanced chiral preference of the asp derivative **3** relative to the ala and leu derivatives **1** and **2** might suggest the presence of specific noncovalent interactions between the projecting amide groups CH_2CONEt_2 and the molecule's backbone and/or iron(III) center. The even further enhanced optical purity of the glu derivatives **4** and **5** is attributed to the extended amino acid bridges that are likely to lower the strain in the complex.

The complexes derived from the glu binders **4** and **5** may be regarded as polycyclic chelate structures consisting of an array of alternating 5-membered and 12-membered chelate rings (Figure 5). The preponderance of the Δ configuration in the glu derivative **4**, and by analogy preponderance of the Λ configuration in the glu derivative **5**, implies a pronounced energy difference between axially and equatorially positioned side chains. In the complexes derived from α-amino acids, the polycyclic structures consist of an array of alternating 5-membered and 10-membered chelate rings. The small chiral preference for either of the diastereoisomers implies minute energy differences between axially and equatorially positioned substituents. This rationale is supported by experimental data on the stereoselectivity of alkylation reactions in 12- and 10-membered macrocyclic ketones and lactones.[37] While the degree of stereoselectivity proved high

(34) Breitmaier, E.; Voelter, W. *Carbon-13 NMR Spectroscopy*; VCH Verlagsgesellschaft mbH: D-6940 Weinheim, Germany, 1987.
(35) Cooney, R. P.; Reid, E. S.; Hendra, P. J.; Fleischmann, M. *J. Am. Chem. Soc.* **1977**, *99*, 2003.
(36) The preference for the Δ configuration in the L-ala and L-leu derivatives **1** and **2** was derived from the positive Cotton effects of their iron(III) complexes around 240 nm.
(37) Still, W. C.; Galynker, I. *Tetrahedron* **1981**, *37*, 3981.
(38) Even at high concentrations of acetate (0.1–0.5 mol L^{-1}) no competition with the scavenger CDTA (10^{-3} mol L^{-1}–10^{-4} mol L^{-1}) is likely to occur at equilibrium conditions, because of the remarkable superiority of CDTA as an Fe(III) binder: Fe(III) acetate,[39] log K = 8.7; Fe^{III}CDTA,[40] log K = 26.9 (both in water).
(39) Somer, L.; Pliska, K. *Coll. Czech. Chem. Commun.* **1961**, *26*, 2754.
(40) Radahkrishran, T. P.; Saraiya, S. C.; Sundaram, A. K. *Curr. Sci.* **1963**, *32*, 450.

Table IV. ^{13}C-NMR Spectral Data for Ferrioxamine Analogs[a]

	compd			
	1	2	3	4
-CON	175.12	175.29		175.01
	174.75	174.72		174.88
	174.55	174.56		
	173.54	173.66	173.57	173.69
	173.30	173.51	173.37 (ms)	173.60
	173.21		172.84	173.12
			172.69	
			171.09	
			170.94	
-COOtBu	?	158.08	157.58	157.78
$-OC(CH_3)$	80.477	80.38	80.62	80.49
$-OCH_3$	52.328	52.318	52.33	52.303
-NHCH-	48.0862	50.80	49.682	51.433
	47.4125	49.935		50.305
	47.2900	49.832		
$-NOHCH_2-$	46.9182	46.71	46.76	46.107
	46.7827	46.63		46.233
	45.6027	45.58	45.52	
$N(CH_2-)_2$			43.522	43.258
			43.449	43.176
			43.423	
			41.621	41.872
			41.539	41.811
$-CH_2-$(leu)		41.47		
		40.825		
$-CH_2-$(asp)			36.19	
			35.59	
$-CH_2CO-$	34.467	34.4122	34.464	34.526
	34.388			
	32.332	32.3348	32.24	32.409
$-CH_2CO-$(glu)				29.151
				29.040
$C(CH_3)_3$	28.769	28.7773	28.768	28.755
$-CH_2-$(glu)				28.428
				28.030
$-CH(CH_3)_2-$(leu)		26.118		
		23.794		
		21.681		
		21.580		
$-CH_3$(ala)	17.464			
	46.898			
	16.806			
$-N(-CH_3)_2$			14.40	14.730
			14.28	14.650
			13.28	13.195

[a] Concentration 20 mM in CD_3OD.

in the former, it became considerably lower in the latter. These observations reflect high energy penalties for placing substituents in axial rather than equatorial positions of 12-membered rings but lower penalties when doing so in 10-membered rings. Force field calculations are currently in progress in an attempt to rationalize the experimental findings.

The high optical purity of **4-Fe(III)** encouraged us to synthesize its enantiomer, namely **5**, as a chiral probe. The latter compound, **5**, was identical in every respect with the corresponding ferrioxamine analogs derived from L-glutamic acid, **4**, except for the CD spectrum of its iron(III) complex, which showed opposite Cotton effects ($\Delta\epsilon$ = -6.7 and +4.5 at 372 and 450 nm, respectively). This mirror image relationship between the enantiomeric trishydroxamate iron(III) complexes **4-Fe(III)** and **5-Fe(III)** confirms the optical purity of the compounds and the lack of any significant racemization during their synthesis.

Using excess CDTA as scavenger and monitoring the iron(III) exchange reaction at a fixed wavelength of 425 nm, an exponential decay of the absorbance with time was observed for all compounds examined. The values of the apparent first-order rate constants obtained, k_{obs}, are presented in Table V.

Linear relationships between the experimental values k_{obs} and the CDTA concentrations used in excess were observed for each

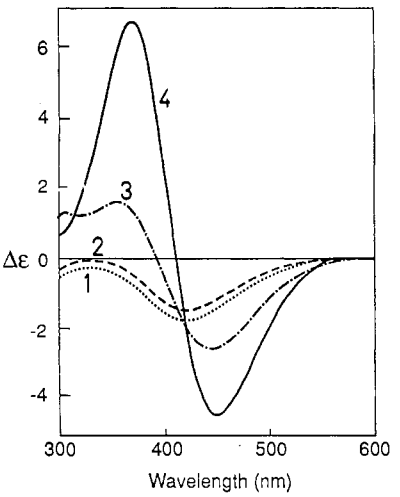

Figure 4. CD spectra of the iron(III) complexes of the biomimetic ferrioxamine analogs: **1** (···); **2** (- - -); **3** (- · -); **4** (—). Solvent: methanol–0.1 N aqueous sodium acetate (4:1). Complex concentrations: (1.5–3.0) × 10^{-2} mol L^{-1}.

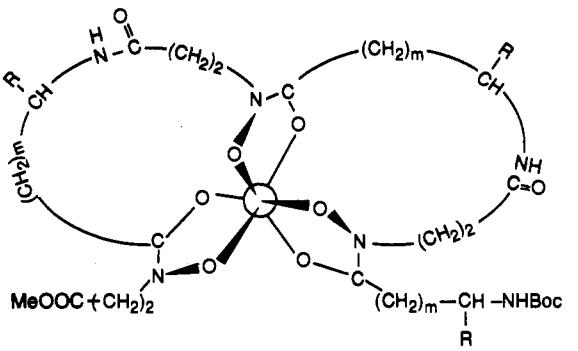

Figure 5. Schematic representation of iron(III) complexes formed from the biomimetic ferrioxamine B analogs.

complex:

$$k_{obs} = k_1[CDTA]_0 + k_2 \quad (2)$$

Here k_1 = second-order rate constant (mol^{-1} L s^{-1}) and k_2 = first-order rate constant (s^{-1}).

The values determined for the kinetic parameters k_1 and k_2 are summarized in Table VI. For the iron(III) complex of ligand **4** and ferrioxamine **B**, the k_2 values became too small to be determined. The experimental data established the following rate law:

$$v = -d[Fe^{III}]/dt = \{k_1[CDTA] + k_2\}[LFe^{III}] \quad (3)$$

The k_1 values decreased with decreasing concentrations of H^+, indicating participation of more than one protonated form of CDTA in the activated complex.[41]

This kinetic equation suggests a dissociation mechanism that involves two processes: (i) a bimolecular step with a second-order rate constant k_1 which depends on the nature of the scavenger and reflects the stability of the iron(III) complex; (ii) a monomolecular step with a first-order rate constant k_2, which measures the inertness of the complex under our experimental conditions (methanol/water, 80:20 by volume; -log $[H^+]$ = 6.3 ± 0.1; I = 0.1). This mechanism is in agreement with the proton-assisted iron(III) ligand exchange reaction observed by Tufano and Raymond.[20]

In order to evaluate the effect of the proton and acetate concentrations on the iron(III) exchange process, we chose to vary the acidity and buffer concentrations for two of the complexes, **1-Fe(III)** and **3-Fe(III)**.[38] The kinetic parameters obtained under

(41) Crumbliss, A. L. *CRD-Handbook of Microbial Iron Chelates*; Winkelmann, G., Ed.; CRC Press, Inc.: Boca Raton, FL, 1991; 177.

Table V. Apparent First-Order Rate Constants[a]

10^3-[CDTA]$_0$ (mol L^{-1})	$10^3(k_{obs} \pm 2\sigma)$ (s^{-1})			$10^6(k_{obs} \pm 2\sigma)$ (s^{-1})	
	1–Fe(III)	2–Fe(III)	3–Fe(III)	4–Fe(III)	ferrioxamine B
0.72	3.79 ± 0.06				
1.48	4.65 ± 0.06	1.88 ± 0.02	0.30 ± 0.01	2.2 ± 0.4	
2.03				3.9 ± 0.4	
2.43	6.0 ± 0.2	2.61 ± 0.04			
2.92		2.91 ± 0.04	0.45 ± 0.01	6.1 ± 0.4	2.6 ± 0.1
3.04			0.50 ± 0.02		
3.46	7.4 ± 0.2				2.3 ± 0.2
3.65			0.54 ± 0.02	7.5 ± 0.6	2.8 ± 0.4
4.65			0.64 ± 0.02	9.3 ± 0.6	
4.75		4.26 ± 0.06			
4.99		4.44 ± 0.04		10.2 ± 0.2	4.0 ± 0.2
5.05	9.1 ± 0.2		0.72 ± 0.02		4.3 ± 0.4
6.70	10.9 ± 0.2				

[a] Solvent methanol/water (80:20); –log [H$^+$] = 6.3 ± 0.1; I = 0.1; T = 25.0 ± 0.1 °C. [**1–Fe(III)**]$_0$ = 1.02 × 10^{-4} mol L^{-1}; [**2–Fe(III)**]$_0$ = 9.55 × 10^{-5} mol L^{-1}; [**3–Fe(III)**]$_0$ = 1.02 × 10^{-4} mol L^{-1}; [**4–Fe(III)**]$_0$ = 1.19 × 10^{-4} mol L^{-1}; [ferrioxamine B]$_0$ = 1.22 × 10^{-4} mol L^{-1}.

Table VI. Kinetic Parameters k_1 and k_2[a]

complex	$k_1 \pm 2\sigma$ (mol^{-1} L s^{-1})	$k_2 \pm 2\sigma$ (s^{-1})
1–Fe(III)	1.20 ± 0.09	(3.0 ± 0.3) × 10^{-3}
2–Fe(III)	(7.2 ± 0.2) × 10^{-1}	(8.1 ± 0.6) × 10^{-4}
3–Fe(III)	(1.1 ± 0.1) × 10^{-1}	(1.3 ± 0.5) × 10^{-4}
4–Fe(III)	(2.0 ± 0.1) × 10^{-3}	
ferrioxamine B	(8.2 ± 0.6) × 10^{-4}	

[a] Solvent methanol/water (80:20); (–log [H$^+$] = 6.3 ± 0.1; I = 0.1; T = 25.0 ± 0.1 °C.

Table VII. Kinetic Parameters k_1 and k_2 under Different Experimental Conditions

complex	–log [H$^+$]	I	$k_1 \pm 2\sigma$ (mol^{-1} L s^{-1})	$k_2 \pm 2\sigma$ (s^{-1})
1–Fe(III)	5.3 ± 0.1	0.1	2.4 ± 0.8	(10 ± 2) × 10^{-3}
	6.4 ± 0.1	0.1	1.20 ± 0.09	(3.0 ± 0.3) × 10^{-3}
	6.9 ± 0.2	0.1	(6.5 ± 0.7) × 10^{-1}	(6 ± 3) × 10^{-4}
	6.4 ± 0.1	0.5	(9 ± 5) × 10^{-1}	(7 ± 2) × 10^{-3}
3–Fe(III)	5.3 ± 0.1	0.1	(5.0 ± 0.6) × 10^{-1}	(1.3 ± 0.2) × 10^{-3}
	6.3 ± 0.1	0.1	(1.1 ± 0.1) × 10^{-1}	(1.3 ± 0.5) × 10^{-4}
	6.8 ± 0.2	0.1	(3.6 ± 0.7) × 10^{-2}	(1.3 ± 1) × 10^{-5}
	6.4 ± 0.1	0.5	(3.5 ± 0.1) × 10^{-1}	(8 ± 4) × 10^{-4}

[a] Solvent methanol/water (80:20); T = 25.0 ± 0.1 °C.

the different conditions are presented in Table VII. The k_2 values decrease with decreasing proton concentrations, in agreement with proton participation in the iron(III) release process. The k_2 values do not vary significantly with the buffer concentrations, when variations of the ionic strength and experimental errors are taken into account. The monomolecular rate constants k_2 were found to increase linearly with the proton concentrations:

$$k_2 = k_H[H^+] \quad (4)$$

Here k_H = second-order rate constant (mol^{-1} L s^{-1}).

In spite of the narrow range of the proton concentrations examined (due to experimental considerations), the k_H values determined for two of the complexes

1–Fe(III)	**3–Fe(III)**
$k_H = (2.0 \pm 0.3) \times 10^3$ mol^{-1} L s^{-1}	$k_H = (2.6 \pm 0.1) \times 10^3$ mol^{-1} L s^{-1}

are comparable with the acidic dissociation rate constants obtained in water for ferrioxamine B[42,43] (k_H = 3.8 × 10^2 mol^{-1} L s^{-1}) or for the tris(acetohydroxamato) iron(III) complex[44] (k_H = 9.9 × 10^4 mol^{-1} L s^{-1}). These results suggest that the k_2 values

Table VIII. Ligand-Exchange Kinetics with EDTA for Ferric Complexes Formed with Linear Trishydroxamate Ligands[a]

ligands	exptl conditions	rate consts
desferrioxamine B	water,[19] pH = 4.3 (acetate), I = 2.0	k = 1.6 × 10^{-2} mol^{-1} L s^{-1}
	water,[20] pH = 5.4 (Tris-acetate), I = 0.1, [EDTA]$_0$ = 8.3 × 10^{-3} mol L^{-1}	k_{obs} = 4.8 × 10^{-5} s^{-1}
	water,[47] pH = 5.3 (acetate), 3.2 × 10^{-4} M ≤ [EDTA]$_0$ ≤ 8.3 × 10^{-3} M	k_{obs} = 7.1 × 10^{-5} s^{-1}
retro-trishydroxamate synthetic analog of desferrioxamine B	water,[47] pH = 5.3 (acetate), 3.2 × 10^{-4} M ≤ [EDTA]$_0$ ≤ 8.3 × 10^{-3} M	k_{obs} = 7.8 × 10^{-5} s^{-1}

[a] T = 25.0 ± 0.1 °C.

determined in this work are related to the acidic dissociation constants observed earlier for the dissociation of the first hydroxamate of ferrioxamine B[42,43] and other bacterial siderophores.[45] The rate law (3) and the above observations are suggesting the following mechanism for iron(III) release from the four synthetic trishydroxamate complexes and from ferrioxamine B under our experimental conditions:

$$H^+ + LFe(III) + CDTA \underset{}{\overset{k_1}{\rightleftharpoons}} CDTAFe(III) + L + H^+$$
$$\searrow^{k_2} \qquad \nearrow_{fast}$$
$$LHFe(III)^+ + CDTA \quad (5)$$

The fast equilibrium proposed in this mechanism has already been measured for monoprotonated ferrioxamine B exchange reactions with EDTA.[20] In order to compare our results with the data available in the literature for the natural ferrioxamine B[19,20] and for a linear trishydroxamate analog,[46] we summarized the data obtained in water with EDTA as scavenger in Table VIII.

It is interesting to note in Table VIII that the inversion of the hydroxamate directionality does not significantly affect the kinetic values. Thus the linear retro-ferrioxamine B analog[46] was reported to show iron(III) exchange parameters similar to those of ferrioxamine B. We however observed 2 orders of magnitude lower dissociation constants for ferrioxamine B in our conditions than in those reported in the literature. This can be attributed to three factors: (i) decreased solvation in aqueous methanol relative to water, (ii) enhanced rigidity of CDTA relative to EDTA, and (iii) lower proton concentrations.

The differences of the kinetic parameters for the synthetic trishydroxamates derived from α-amino acids possessing the same chain length, namely ligands **1–3**, could be attributed to differences in the substituents R and their electron-donating properties and bulkiness (Table VI). The electron-donating properties of the substituents R may thus affect the binding properties of the hydroxamate coordination sites, as previously observed[47–49] for differently substituted hydroxamic acids. According to these results, the greatest effect is due to the nature of the substituents R_2 on the nitrogen atom of the hydroxamate function (structure I). In this work, the only effect could be due to changes in the electronic properties of substituents on the carbon atom of the hydroxamate group (R_1 in structure I). The inductive electron donor ability of the substituents R increases when R = CH_2-

(42) Monzyk, B.; Crumbliss, A. L. *J. Am. Chem. Soc.* **1982**, *104*, 4921.
(43) Birus, M.; Bradic, Z.; Krznaric, G.; Kujundzic, N.; Pribanic, M.; Wilkins, P.; Wilkins, R. *Inorg. Chem.* **1987**, *26*, 1000.
(44) Birus, M.; Bradic, Z.; Kujundzic, N.; Pribanic, M.; Wilkins, P.; Wilkins, R. *Inorg. Chem.* **1985**, *24*, 3980.
(45) Abdallah, M.; Albrecht-Gary, A. M.; Blanc, S.; Linget, C.; Roedel, M. *Proceedings of the XXVII International Conference on Coordination Chemistry*; Gera, Germany, 1990; Vol. 1, p 66.
(46) Shimizu, K.; Akiyama, M. *J. Chem. Soc., Chem. Commun.* **1985**, 183.
(47) Monzyk, B.; Crumbliss, A. L. *J. Am. Chem. Soc.* **1979**, *101*, 6203.
(48) Fish, L. L.; Crumbliss, A. L. *Inorg. Chem.* **1985**, *24*, 2198.
(49) Brink, C. P.; Crumbliss, A. L. *Inorg. Chem.* **1984**, *23*, 4708.

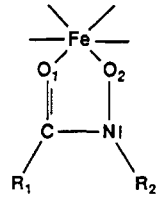

1

$CONEt_2$ is replaced by Me and *i*-Bu. This should increase the protonation constants and the stability of the ferric complexes and decrease the values of our k_2 rate constants according to literature data.[47-49] Our results deviate from this trend, indicating predominant contributions of other factors (Table VI). One of these factors is likely to be the bulkiness of the substituents R (Figure 2). Increased steric hindrance in the formation of the activated complex with CDTA is contributing to the decrease in the second-order rate constants k_1 by 1 order of magnitude when R = Me is replaced by *i*-Bu and CH_2CONEt_2 (Table VI).

More dramatic changes of the rates of dissociation are observed when there is an increase in the chain length of the amino acid between the hydroxamate groups in the ligand. Comparing ligand **3** with ligand **4** reveals a decrease of about 2 orders of magnitude for the bimolecular rate constant k_1. It is also remarkable to note that the second-order rate constant k_1 for the biomimetic ligand **4** is very close to that of the natural ferrioxamine B (Table VIII). The kinetic parameters of the biomimetic ferric complexes thus become comparable with those of the natural ferrioxamine B as the chain length increases and the strain diminishes.

Summary and Conclusion

A novel series of synthetic trishydroxamates has been prepared that, similarly to the natural ferrioxamine, bind iron(III) in a 1:1 stoichiometry. Due to the presence of asymmetric carbons the synthetic binders differ from the natural compound in forming complexes of preferred chiral sense. Quite pronounced differences were observed in the chiral purity of the synthetic iron(III) complexes. In the ala and leu derivatives **1** and **2** the chiral preference for the Δ configuration was rather modest, indicating minute energy differences between the two possible diastereoisomers. In the asp derivative **3**, on the other hand, and particularly in the glu derivative **4**, the chiral preference for the Δ configuration when using the natural L-glutamic acid was remarkable, reflecting significant enhancement of the energy gap between the two possible isomers.

The iron(III) complexes of the α-amino acid derivatives **1–3** dissociate significantly faster than the complex of the glu derivative **4**. This is attributed to the presence of strain in the former three, which is released when the amino acid links are lengthened by two methylene groups in the latter **4**. The lower kinetic rate constants k_1 and k_2 of the asp derivative **3** relative to the ala and leu derivatives **1** and **2** suggest the presence of stabilizing, noncovalent interactions between the amide side chains and the molecules' backbone and/or iron(III) center. Such interactions could also account for the higher chiral preference of the **3–Fe(III)** complex relative to **1–Fe(III)** and **2–Fe(III)**.

This work also illustrates the effect of steric hindrance on ligand-exchange rates. The second-order k_1 values decreased by about 1 order of magnitude in the series **1–Fe(III)** > **2–Fe(III)** > **3–Fe(III)**. The most pronounced effect was however observed in the glu derivative **4–Fe(III)**, which showed a decrease of the bimolecular ligand exchange process by about 3 orders of magnitude relative to **1–Fe(III)**. The kinetic behavior of **4–Fe(III)** could be attributed to both the steric hindrance imposed by the $CONEt_2$ side chain and the low strain of its polycyclic system, which becomes resistant toward attack by scavenger (k_1) and proton (k_2).

Although the lower homologs **1–3** are substantially different from the natural ferrioxamine B in terms of their coordination properties, they fully reproduce the activity of the natural siderophore in vivo as growth promoters and iron(III) carriers in two types of microorganisms.[13-15] The higher homologs **4** and **5**, which are significantly closer to ferrioxamine B in their iron(III) release kinetics, behave differently in the two types of organisms. Thus both isomers **4** and **5** substitute ferrioxamine B in *E. herbicola*,[14] irrespective of their chirality. In *P. putida*, however, the glu derivatives **4** and **5** merely bind to the respective receptor without transversing the microbial membrane, with the glu derivative **5** of Λ configuration being 3-fold more effective than the glu derivative **4** of Δ configuration.[15]

These findings suggest that the transport of the siderophore iron(III) complex across the membrane is the determinant factor in these compounds' biological activity. They further illustrate the role of conformational subtleties in determining in vivo activity, indicate the pronounced differences between related siderophore receptors of different organisms, and demonstrate the usefulness of structurally and physicochemically fully characterized synthetic siderophore analogs as probes of microbial iron(III) uptake systems.

Acknowledgment. The authors thank Dr. Alain van Dorsselaer and Sylvie Kieffer for helpful discussions and FAB mass spectrometric measurements, Mrs. R. Lazar for her skillful technical assistance, and the U.S.-Israel Binational Science Foundation and the CNRS-France for financial support. A.S. is the holder of the Siefried and Irma Ullmann professorial chairs.